High-resolution simulation of link-level vehicle emissions and concentrations for air pollutants in a traffic-populated East Asian city

Shaojun Zhang [1, 2], Ye Wu [1, 3 *], Ruikun Huang [1], Jiandong Wang [1], Han Yan [1], Yali Zheng [1, 4], Jiming Hao [1, 3]

1 School of Environment and State Key Joint Laboratory of Environment Simulation and Pollution Control, Tsinghua University, Beijing 100084, China, Tsinghua University, Beijing 100084, P. R. China

[2] Department of Mechanical Engineering, University of Michigan, Ann Arbor, MI 48109, U.S.

[3] State Environmental Protection Key Laboratory of Sources and Control of Air Pollution Complex, Beijing 100084, P. R. China

[4] Society of Automotive Engineers of China, 102 Lianhuachi East Road, Beijing 100055, P.R. China

Correspondence to: Y. Wu (ywu@tsinghua.edu.cn)

Abstract:

Vehicle emissions of air pollutants created substantial environmental impacts on air quality for many traffic-populated cities in East Asia. A high-resolution emission inventory is a useful tool compared with traditional tools (e.g., registration data based approach) to accurately evaluate real-world traffic dynamics and their environmental burden. In this study, Macao, one of the most populated cities in the world, is selected to demonstrate a high-resolution simulation of vehicular emissions and their contribution to air pollutant concentrations by coupling multi-models. First, traffic volumes by vehicle category on 47 typical roads were investigated during weekdays of 2010 and further applied in a networking demand simulation with the TransCAD model to establish hourly profiles of link-level vehicle counts. Local vehicle driving speed and vehicle age distribution data were also collected in Macao. Second, based on a localized vehicle emission model (e.g., the EMBEV-Macao), this study established a link-based vehicle emission inventory in Macao with high resolution meshed in a temporal and spatial framework. Furthermore, we employed the AERMOD model to map concentrations of CO and primary $PM_{2.5}$ contributed by local vehicle emissions during the weekdays of November 2010. This study has discerned the strong impact of traffic flow dynamics on the temporal and spatial patterns of vehicle emissions, such as a geographic discrepancy of spatial allocation up to 26% between THC and $PM_{2.5}$ emissions owing to spatially heterogeneous vehicle-use intensity between motorcycles and diesel fleets. We also identified that the estimated CO_2

emissions from gasoline vehicles were in a nice agreement with the statistical fuel consumption in Macao. Therefore, this paper provides a case study and a solid framework for developing high-resolution environment assessment tools for other vehicle-populated cities in East Asia.

1. Introduction

The soaring vehicle stock driven by social-economic development has created a series of substantial challenges regarding air pollution, energy insecurity, and public health within many countries (Uherek et al., 2010; Saikawa et al., 2011; Shindell et al., 2011; Walsh, 2014). At the national level, we take nitrogen oxides (NO_X) emissions as an example as it is an essential precursor to the formation of ozone and nitrate aerosol in the atmosphere. On-road vehicles are currently responsible for 29% of national anthropogenic NO_X emissions in China (MEP, 2014), 37% in U.S. (U.S. EPA, 2014) and 40% in Europe Union (EEA, 2014; Vestreng et al., 2009). At the city level, the vehicular contribution to ambient nitrogen dioxide (NO_2) concentration is very significant in traffic related areas (Carslaw et al., 2011). For example, in European countries where diesel vehicles make up a considerable part of private passenger cars, near-road NO_2 concentration exceeds the ambient air quality standard. This issue is seen as one of the most significant air pollution problems in Europe although great efforts have been made to cope with the NO_2 exceedance, including the implementation of stringent emission standards for diesel vehicles (e.g., the latest Euro 6 requirements) (Franco et al., 2014; Carslaw et al., 2011; Carslaw and Rhys-Tyler, 2013; Chen and Borken-Kleefeld, 2014). Higher health risk as a result of exposure to vehicular emissions (e.g., particle, NO_X) is understandable in traffic-populated cities, and is probably associated with the large resident population, greater traffic congestion and unfavorable dispersion due to dense buildings (Du et al., 2012; Ji et al., 2012). In 2012, the International Agency for Research on Cancer Group 1 assessed the carcinogenicity of diesel emissions as "carcinogenic to humans" with sufficient evidence for it to be characterized as a cause of lung cancer (Benbrahim-Tellaa et al., 2012).

The high-resolution vehicle emission inventory can be a valuable tool to accurately evaluate impacts on air quality and public health, as it can well reflect the close connections between environmental impacts and traffic flows. McDonald et al. (2014) analyzed the impacts of enhanced spatial resolution from 10 km to 500 m on vehicular CO_2 emission inventory for Los Angeles, which clearly demonstrated substantial improvements in the accuracy for areas containing traffic-dense microenvironments (e.g., heavily trafficked highways). Consequently, link-based emission inventory is a preferred tool owing to its substantial advantage in spatial resolution for local traffic and environmental management. Over the past

decade, high-resolution emission inventory initiatives have been carried out in China's vehicle-populated cities. Taking Beijing, the capital city of China for example, Huo et al. (2009) established a link-based emission inventory for light-duty gasoline vehicles (LDGVs) in the urban area based on estimated emission factors with the IVE model. However, significant emissions of NO_X and fine particulate matter ($PM_{2.5}$) may be attributed to heavy-duty diesel vehicles (HDDVs) instead of LDGVs, including the gross emitters registered in other provinces (Wang et al., 2011 and 2012a), whose contributions are currently not evidenced in the registration-based inventories for China's vehicle-populated cities (Wu et al., 2011; Zhang et al., 2014a; Zheng et al., 2014). Wang et al. (2009) and Zhou et al. (2010) estimated vehicular emissions for the urban area of Beijing by using grid-based data of average speed and aggregated vehicle kilometers travelled. However, their resolutions are not sufficient to present hourly fluctuation of network traffic volume and quantify vehicular emissions at the link level.

As traffic management actions become more important for vehicle emission control, such as the license control policies effective in seven vehicle-populated cities of China (e.g., Shanghai, Beijing, Guangzhou, Tianjin, etc.) and the Electronic Road Pricing (ERP) program adopted in Singapore (Goh, 2002). We therefore envision greater demand for high-resolution vehicle emission inventories by local environmental protection administrations in the near future. A few technical barriers are expected to be shortly overcome for improving the high-resolution vehicular emission inventory based on the development experience of the London Atmospheric Emission Inventory (LAEI) (TfL, 2014). First, high-resolution traffic data including traffic counts, vehicle speed and fleet composition should be investigated or estimated at the link level with hourly fluctuations. Second, real-world emission factors should be developed based on a sufficient measurement database to effectively address potential uncertainties (e.g., gaps between regulatory cycle and off-cycle conditions) (Carslaw et al., 2011; Wu et al., 2012; Zhang et al., 2014a). Third, technology allocations of the total fleet (e.g., traffic counts by fuel type and vehicle age) should be derived based on real-world traffic data instead of registration data, considering vehicular emissions are fairly sensitive to vehicle technology allocations (Vallamsundar and Lin, 2012). Finally, the application of high-resolution emission inventory can be significantly enhanced by extending the evaluation framework from vehicular emissions to pollutant concentration, which are of overriding concerns to residents, pedestrians and policy-makers (Vallamsundar and Lin, 2012; Misra et al., 2013).

In this study, we selected Macao as a case city to demonstrate high-resolution simulation for vehicle emissions and primary concentrations of air pollutants in this traffic-populated city. Macao is well-renowned for its tourism and gaming industry, which attracts numerous visitors and created a large

transportation demand. Owing to the absence of massive rail-based public transit system, which is now under construction in Macao, local transportation completely depends on on-road vehicles. The vehicle-population density (including motorcycles, MCs) in Macao is approaching 7800 veh km^{-2} in 2014, significantly more dense as compared with other East Asian cities (e.g., 430 veh km^{-2} of Shanghai, 340 veh km^{-2} of Beijing and 700 veh km^{-2} of Hong Kong) (DESC, 2014; HKS, 2014; NBSC, 2014). Furthermore, Macao's total vehicle population has surpassed 240 thousand in 2014, more than double the level in 2000 (DESC, 2014). Significant gridlock has been caused due to rapid motorization in the Macao Peninsula during rush hours, when the average speed of arterial roads is frequently lower than 15 km h^{-1} (TMB, 2010). On the other hand, local air quality data indicate several nonattainment sites for annual ambient $PM_{2.5}$ and NO_2 concentrations in the traffic-dense and residential areas of Macao (DESC, 2014). On-road vehicles have been identified as the major local contributor to air pollution, because industrial emissions in Macao are quite minor compared with the on-road transportation sector. Thus, there is an urgent need to attach importance to controlling vehicular emissions with the support of high-resolution emission inventory technology in this traffic-populated city.

2. Methodology and data

2.1 General study framework and components

This study generally consists of three components: (1) characterizing hourly traffic profiles at the link level, (2) establishing a high-resolution vehicle emission inventory, and (3) simulating the concentrations of typical primary air pollutants (e.g., CO, $PM_{2.5}$) contributed by local vehicle emissions in Macao (see Fig. 1). The core task of this study is to calculate emissions of air pollutants and carbon dioxide (CO_2) from local vehicles meshed in the high resolution matrix of the "hour-link-vehicle technology group", which is illustrated by Equation 1.

$$E_{h, l, p, v} = \sum_{f, y} 10^{-3} \cdot EF_{f, p, v, y} \cdot L_l \cdot TV_{h, l, v} \cdot VF_{f, v, y} \quad (1)$$

where $E_{h, l, p, v}$ are the emissions of pollutant category p from vehicle classification v during hour h for link l, kg h^{-1}; $EF_{f, p, v, y}$ is speed-dependent average emission factor of pollutant category p for vehicle technology group defined by classification v, fuel type f and vehicle age y, g veh^{-1} km^{-1}; L_l is the total length of link l, km; $TV_{h, l, v}$ is total traffic volume of vehicle classification v during hour h, veh h^{-1}; and $VF_{f, v, y}$ is the volume fraction of vehicle technology group (e.g., model year group) defined by fuel type

f and vehicle age y. We define eight vehicle classifications in this study that were recognized from road traffic video records as follow: light-duty passenger vehicle (LDPV), MC, taxi, public bus (PB), medium-duty passenger vehicle (MDPV), heavy-duty passenger vehicle (HDPV), light-duty truck (LDT) and heavy-duty truck (HDT).

Therefore, we further characterized total hourly emissions from the total vehicle fleet based on the bottom-up method, namely from each link to the entire road net, as Equation 2 illustrates.

$$E_{h, p} = \sum_{l, v} E_{h, l, p, v} \qquad (2)$$

where $E_{h, p}$ are the total vehicle emissions of pollutant category p during hour h from the total vehicle fleet in Macao, kg h^{-1}. In the following two sub-sections, we present detailed methods for developing high-resolution traffic data and vehicle emission factors. Due to the time limitation on the traffic field investigation, we only focus the case study for weekdays during 2010; weekends were not investigated when traffic flows might be different.

2.2 Summary of geography and road network in Macao

Macao is one of the two Special Administrative Regions (SAR) in China lies on the western side of the Pearl River Delta, with a total land area of only 30 km^2, which is the most densely populated city in the world (~20 thousand people km^2) (DSEC, 2014). The Macao SAR now consists of the Macao Peninsula (MP) and the Taipa-Cotai-Coloane (TCC) islands (See Fig. S1). In particular, the CoTai Reclamation Area is a piece of newly reclaimed land on the top of the bay area between Taipa and Coloane, where new casinos and hotels have been constructed since land of Macao is scare. Nearly 90% of Macao's total population is concentrated in the MP, where the population density is significantly higher than the combined density of Taipa-CoTai-Coloane (TCC) regions (i.e., 54 thousand vs. 4.3 thousand, unit in people km^{-2}). The MP geographically consists of five regions, nominally parishes. Among those five parishes, the St. Anthony Parish where the Ruins of St. Pual's Cathedral is located has the highest population density, which is approaching 120 thousand people km^{-2}.

Based on the GIS database of road network in Macao provided by the Macao Transportation Bureau, there were a total of 1704 road links in the study year of 2010. We categorized all those links into three road classes: urban freeways, arterial roads and residential roads, representing that the level of service decreasing from high to low. It should be noted that the road links are unevenly distributed among various

areas of Macao, but similar to the spatial patterns. For example, 77% of all road links (i.e., 1306 links) were concentrated in the Macao Peninsula, which were responsible for 59% of Macao's total road length.

2.3 Field investigation and simulation of link-based traffic data

We investigated traffic data on 47 typical road links during three field investigation periods from Jan 2010 to Jan 2011 (i.e., nearly 20 weekdays during Jan 2010, May 2010 and Jan 2011) (see Fig. S2), according to the spatial heterogeneity of road network in Macao by covering all road classes and regions. The length coverage proportion of urban freeways was higher than that for arterial and residential roads, because of higher traffic volumes on the urban freeways. The real traffic flow records of each link was collected with a portable video camera for at least 20 minutes within each hour. Among all links investigated, 5 typical road links varying in road classes (1 freeway, 2 arterial roads and 2 residential roads) were investigated for the entire day (i.e., 24-h sampling). Sampling duration for the rest of the links investigated in general were from 6 a.m. to 11 p.m. (i.e., day-time sampling). Detailed hourly traffic volumes by vehicle classification for 47 road links were further broken down based on those original video profiles by major region and road class (see Table 1). We can clearly observe variations in hourly total traffic counts for three road classes, with significant peaks of traffic demand during morning and evening rush hours (see Fig. 2 and Table 1).

Traffic volume fraction by vehicle classification is another essential type of data obtained from traffic video record (see Fig. S3 as an example of arterial roads). During the evening rush hour (6 p.m.), LDPVs and MCs contributed nearly 80% of total traffic volume, which are the two major vehicle types used for daily commuting demand in Macao. In particular, MCs are low-cost commuting vehicles for the relatively lower income group in Macao. Therefore, the observed traffic fraction of MCs (~45%) was higher than that of LDPVs (~35%) on arterial roads of the Macao Peninsula. By contrast, observed traffic fraction of MCs in the TCC was only approximately 15%. In addition to the spatial variations among various road classes and areas, we also observed temporal variations of various vehicle classifications. Taking arterial roads in the MP for example, their average traffic fractions of taxis were approximately 10% during the day time (6 a.m. to 12 p.m.). During the night time (12 p.m. to 6 a.m.), accompanied by significantly reduced traffic demand of MCs and LDPVs, taxis could be responsible for 20~30% of total vehicle counts. Due to the minor economic contribution of local industry, the average traffic fraction of trucks in Macao indicating freight transportation was significantly lower than those in Beijing and

1   Guangzhou. Furthermore, for the other road links without observed traffic fraction data, we used the

2   hourly and area aggregated proportions for further modeling (see Equation 3).

3 $$\overline{VF}_{a, c, h, v} = \frac{1}{N_{TV\ a, c, h, v}} \sum_{l \in (a,\ c)} VF_{a, c, h, l, v} \quad (3)$$

4   where $\overline{TF}_{a, c, h, v}$ is average traffic volume fraction for area a, road class c, hour h, and vehicle classification

5   v; $N_{TV\ a, c, h, v}$ is the number of road links with the investigated traffic volume available for area a, road

6   class c, hour h, and vehicle classification v; $VF_{a, c, h, l, v}$ is the average traffic volume fraction for hour h,

7   road link l and vehicle classification v and the link is in area a and under the road class c.

8   The TransCAD 5.0 model was applied to estimate total traffic demand and its spatial allocation at

9   the link level. TransCAD 5.0, one of the most widely-used traffic planning software, can estimate origin-

10   destination (OD) matrix of the road network from link traffic counts. In this study, we selected the multiple

11   path matrix estimation (MPME) procedure provided by the TransCAD 5.0 and estimated total traffic

12   volumes of all road links during the 6 p.m. hour with observed hourly traffic counts of 33 links as input

13   data. After a number of iteration runs, the average discrepancy between simulated traffic volumes and the

14   observed values (i.e., output vs. input) is 4.3% and the Pearson coefficient is 0.95, indicating statistically

15   satisfactory results (see Fig. S4). We could identify wide variations in hourly traffic activity among

16   individual roads of one road class group (see Fig. 2), and the variations may attributed to the difference in

17   the designed traffic capacity (e.g., number of lanes) and location. In terms of the hourly allocation of

18   traffic volume, which is a non-dimensional indicator of temporal variability, the results could indicate nice

19   consistency among individual roads with much lower variations (see Fig. S5). Therefore, for other hours,

20   we estimated hourly total traffic volumes based on the averaged temporal allocations and simulated traffic

21   volumes during the 6 p.m. hour, as Equation 4 illustrates.

22 $$TV_{h, 1} = TV_{18, 1} \cdot \frac{\overline{\alpha_{a,c,h}}}{\alpha_{a, c, 18}} \quad (4)$$

23   where $TV_{h, 1}$ is the hourly total traffic volume for road link l during the hour h, veh h^{-1}, and $TV_{18, 1}$ is

24   particularly the hourly data during the 6 p.m. hour simulated by the TransCAD if observed traffic volume

25   data is unavailable); $\overline{\alpha_{a,c,h}}$ is the averaged ratio of hourly total traffic volume during the hour h to daily

26   total traffic volume for the area a and the road class c. Therefore, the traffic volumes by vehicle

27   classification are further estimated based on the traffic fraction data averaged by area, road class and hour.

28   The total 24-h traffic activity by vehicle classification can be estimated with Equation 5.

1 $$TA_{daily\ v} = \sum_{h=0}^{23}\sum_{l} TV_{h,l} \cdot L_l \cdot VF_{h,l,v} \qquad (5)$$

2 where $TA_{daily\ v}$ is the daily traffic activity in the entire research domain for vehicle classification v, veh

3 km d^{-1}; $VF_{h,l,v}$ is the hourly traffic volume fraction for hour h, link l and vehicle classification v, and if

4 the $VF_{h,l,v}$ is not available from the traffic field study data, $VF_{h,l,v}$ would be applied by the aggregated

5 data (i.e., $\overline{VF}_{a,c,h,v}$, $l \in (a,\ c)$) that is estimated according to Equation (3)

6   In addition to traffic volume, traffic condition indicated by link-based hourly speed is another

7 category of essential input data. First, we used a portable GPS receiver to collect second-by-second vehicle

8 trajectory data for on-road vehicles during the same field sampling periods of traffic counts. Considering

9 the distinctions of driving behaviors among MCs, PBs and other vehicle classifications (e.g., passenger

10 vehicles and trucks), like more frequent stops for PBs to discharge and receive passengers, we used a taxi

11 equipped with the GPS receiver to chase LDPVs randomly to represent traffic conditions for on-road

12 vehicles other than PBs and MCs. Each targeted vehicle was chased for at least 10 minutes. For PBs and

13 MCs, we selected typical vehicles to record their traffic trajectory data. In this study, we collected traffic

14 trajectory data of LPDVs, PBs and MCs for 32 hours, 24 hours and 8.4 hours, respectively, with high

15 abundance of spatial and temporal distribution. Second, we integrate the original second-by-second GPS

16 trajectory data with the road network GIS system to identify the road link information (e.g., link name,

17 parish and road class) for each sampling second. Third, we estimated averaged hourly speed for each road

18 class in each parish.

19 $$\overline{V}_{a,c,h,v} = \frac{1}{N_{V\ a,c,h,v}} \sum_{l \in (a,\ c)} \overline{V}_{a,c,h,l,v} \qquad (6)$$

20 where $\overline{V}_{a,c,h,v}$ is average hourly speed for road class c, hour h, region r, and vehicle classification v

21 (LDPVs, PBs, and MCs in this equation), km h^{-1}; $N_{V\ a,c,h,v}$ is the number of link with the investigated

22 speed available for road class c, hour h, area a and vehicle classification v; $\overline{V}_{a,c,h,l,v}$ is the average speed

23 for hour h, road link l and vehicle classification v, km h^{-1}, and the link is in area a and under the road class

24 c. Considerable temporal and spatial variability in the hourly speeds across road links remained due to the

25 limited data compared with the vast entire road network. For example, the coefficients of variation for the

26 hourly speeds of arterial roads in the MP were 48%, 40%, and 48%, respectively, during a morning rush

27 hour (14 road samples, 8 a.m.), a noontime hour (16 road samples, 12 noon), and an evening rush hour

28 (13 road samples, 6 p.m.) within a single investigation day. In other cities or regions where intelligent

transportation systems (ITS) are developed, we suggest the application of ITS-informed traffic data to better capture the temporal and spatial traffic heterogeneity among various road links.

To validate the speed profiles, we observed variations in average hourly speeds by area and road class for LDPVs as an example, which were aggregated by link-level speed profiles with traffic volume data taken into account (see Fig. 3). Clearly, average hourly speeds for arterial and residential roads in the MP were lower than 20 km h^{-1} for longer than 15 hours (e.g., from 6 a.m. to 8 p.m.), indicating extremely congested traffic conditions. In particular, average hourly speeds during the evening rush period (e.g., 6 p.m. and 7 p.m.) were even less than 15 km h^{-1}, which corresponded to the officially released data. In the TCC, where traffic is less populated, average hourly speeds for arterial and residential roads were significantly higher than those in the Macao Peninsula, ranging from 20 km h^{-1} to 40 km h^{-1} except for the 6 p.m. hour. On the other hand, we could also observe differences of aggregated daily speed among various vehicle classifications (see Fig. S6). For example, average daily speed of taxis was 24.0 km h^{-1}, higher than the 21.7 km h^{-1} of LDPVs, due to higher traffic volume fraction of taxis in the night time when there were usually free traffic flows. Similarly, average speed of HDTs was 27.0 km h^{-1}, topping all vehicle classifications, because their traffic volume fraction was significantly higher in the TCC compared to the MP.

2.4 Emission factor development and the integration with traffic data and vehicle age distribution

We initiated a comprehensive measurement program of collecting real-world emission profiles since 2010, in order to establish and update a localized emission factor model for vehicles in Macao (e.g., the EMBEV-Macao model). So far, more than 60 typical vehicles, LDPVs, taxis, PBs, LDTs and HDTs, have been measured on road by using a portable emission measurement system (PEMS). Furthermore, a large-scale remote sensing vehicle emission measurement project was conducted during March and April 2008, which enabled the collection of fuel-based emission factors for MCs in Macao. Detailed experimental section in Macao and the measurement results are documented in several of our previous papers regarding gasoline, diesel and more advanced vehicles (e.g., hybrid electric vehicles) (Hu et al., 2012; Wang et al., 2014; Zhang et al., 2014b; Zhou et al., 2014; Wu et al., 2015a and 2015b; Zheng et al., 2015). We developed an emission factor model, the EMBEV-Macao model, with reference to the modeling framework and methodology of the EMBEV model which is originally developed for the vehicle fleet in Beijing (Zhang et al., 2014a). Technically, these two emission measurement methods (PEMS and remote sensing) have their owner useful features and practical limitations for developing emission factors. As for

1 the PEMS testing, it could provide accurate measurement of real-world emissions for an entire trip for
2 each vehicle. However, the PEMS method usually collects limited vehicle samples due to the expensive
3 and time consuming experimental process. In contrast, the remote sensing method could collect large-
4 sized vehicle samples so it is capable of presenting the emission trends over a wide spectrum of model
5 years and vehicle conditions (Zhou et al., 2014; Bishop et al., 2012). However, the short test duration and
6 limited test sites of remote sensing measurements are also questioned for the representativeness of vehicle
7 emissions (Lee and Frey, 2012; Chen and Borken-Kleefeld, 2015). Thus, we attempted to use the
8 advantage of each measurement method to develop local emission factors. Tasking the gasoline LDPVs
9 for example, the remote sensing results indicated that vehicles with model year (MY) later than 2004 have
10 consistently lower gaseous emissions (Zhou et al., 2014), which were comparable to those of modern
11 vehicles complying with the Euro 5 emission standard (Zhang et al., 2014a). We assumed these post-MY
12 2004 gasoline LDPVs as one vehicle age group, and apply the basic emission parameters of the Euro 5
13 for the post-MY 2004 gasoline LDPVs in Macao (e.g., basic emission factors, deterioration rates) with
14 additional modifications. First, we developed localized speed correction curves based on a micro-trip
15 method for each vehicle classification to integrate vehicle emission factors and traffic conditions at the
16 link-level (Zhang et al., 2014b and 2014c; Wu et al., 2015). Second, we used the PEMS results to derive
17 the extra emissions in the start stage, and modified the start emission parameters (e.g., gram per start).
18 Third, the EMBEV-Macao model enables us to correct impacts of local temperature, fuel quality, air
19 conditioning usage, and other aspects to the real conditions. For example, the sulfur content of gasoline
20 and diesel were approximately 90 ppm and 15 ppm during 2010. In addition, the original EMBEV model
21 has already developed detailed distribution functions of emission factors, which can address the effect of
22 high emitters. It is noted several vehicle fleets have limited PEMS or dynamometer test data in China (e.g.,
23 MC), we developed their emission factors mainly based on the remote sensing results (Zhou et al., 2014).

24   Considering that there was no significant policy influencing traffic flow composition during 2008-
25 2010, we estimated detailed traffic fraction by fuel type and vehicle age for each vehicle classification
26 based on the vehicle information database from the 2008 remote sensing project (Zhou et al., 2014). It
27 should be noted that some vehicle classifications have a single fuel type; e.g., gasoline for MCs and diesel
28 for PBs. By contrast, other vehicle specifications like engine displacement have a more important effect
29 on real-world emissions. Therefore, we also derived the on-road traffic volume split ratios by engine
30 displacement for MCs and PBs (refer to the footnote of Table 2). Table 2 illustrates the detailed traffic

1 volume fraction by vehicle age and fuel type (or split by engine displacement for MCs and PBs) for each

2 vehicle classification.

4 **2.5 Modeling dispersion of vehicular air pollutants**

5   Urban air quality models are commonly used to estimate the spatial distribution of vehicular

6 pollutants by simulating their chemical and physical processes in the atmosphere within urban areas.

7 Holmes and Morawska (2006) classified dispersion models into Box models, Gaussian models,

8 Lagrangian models, Computational Fluid Dynamic (CFD) models. Currently, Gaussian models are

9 recommended by the environmental protection agency of most countries all over the world.

10   The AMS/EPA regulatory model (AERMOD) is a steady state Gaussian plume dispersion model

11 which is recommended by U.S. EPA (U.S. EPA, 2004). The modeling system consists of one main

12 program (AERMOD) and two pre-processors (i.e., AERMET and AERMAP). In addition, calculating

13 urban boundary layer parameters and considering urban heat island effect makes AERMOD sensitive for

14 local meteorological conditions. Recently, several studies have investigated the integration performances

15 of the traffic simulation model, vehicle emission model and the AERMOD model. For example,

16 Vallamsundar and Lin (2012) integrated MOVES and AERMOD models to simulate the $PM_{2.5}$ hotspot

17 cases of typical roads in U.S. cities (i.e., study domain area of ~0.5 km^2) and provided some implications

18 based on sensitivity analysis, such as narrowing the data gap between traffic, emissions and air quality

19 models and further investigation of important local input data (e.g., traffic composition, fleet age

20 distribution). Misra et al. (2013) also integrated a traffic simulation model, a vehicle emission model and

21 the AERMOD model to estimate traffic-related pollution in downtown Toronto (i.e., study domain area

22 of ~0.5 km^2). It should be noted that, in those previous investigations at near-field level (Zannetti, 1990),

23 the AERMOD simulated vehicular emissions as a series of point sources which approximate a traffic lane.

24   Considering a significantly larger study area, higher road density and the scarcity of metrological

25 data and surrounding building profiles in a sufficiently fine resolution, we divided the study domain into

26 a grid of 350 square cells (500 m×500 m). Aggregated hourly vehicular emissions of major pollutants

27 (e.g., CO and $PM_{2.5}$) from all road links in each grid are used as the input data for the AERMOD. The

28 receptors are placed at central points of all cells at a height of 2.0 m. In terms of the geographic data and

29 the altitude information is obtained from the Google Earth. Building downwash effects are simulated by

30 the AERMOD. In our study, we model the weekdays of November 2010 when rainy days were much

31 fewer compared to other months. Hourly meteorological profiles from two monitoring sites located in MP

1 and TCC respectively, including temperature, wind direction, wind speed, relative humidity and air

2 pressure are provided by the Department of Metrological Services in Macao. The northeasterly winds are

3 prevailing during that month, supplemented by a minor part of northerly and easterly winds (see Fig. S7).

4   It is noted that the AERMOD has the function of simulate the dispersion of NO_X as well as the

5 oxidation process from freshly emitted NO to ambient NO_2 with simplified chemical mechanisms (U.S.

6 EPA, 2015). For example, the AERMOD considers NO conversion to NO_2 by reaction with ambient ozone

7 (i.e., $NO + O_3 \rightarrow NO_2 + O_2$, which is used by both two EPA Tier 3 methods such as OLM and PVMRM)

8 (U.S. EPA, 2015; Podrez, 2015). However, the NO/NO_2 conversion module of the AERMOD is developed

9 based on simplified mechanism and regressions using historical monitoring data, which may have several

10 limitations compared to actual complex chemistry. First, there are numerous other reactions that would

11 further oxidize NO_2 to other NO_Y species (e.g., nitrate radical, nitrate acid, peroxyacyl nitrates), and

12 Pollack et al (2012) suggest that the production of these NO_Y species may differ by period (e.g., daytime

13 vs. nighttime; weekdays vs. weekends). However, these reactions removing NO_2 from the atmosphere

14 have not been considered by the AERMOD. Second, this basic chemical reaction in the AERMOD (NO

15 $+ O_3 \rightarrow NO_2 + O_2$) is simply assumed to be instantaneous and irreversible on hourly basis (U.S. EPA,

16 2015). The convention ratio is greatly dependent on the ambient ozone concentration (both OLM and

17 PVMRM) and the estimated mixing status of ambient ozone in the plume (PVMRM). However, the spatial

18 distribution of ambient ozone concentration in a city is highly heterogeneous (Murphy et al., 2007), which

19 is a substantial hurdle to assure the simulation accuracy over a city-level area. For these reasons, we didn't

20 include the NO_2 simulation results in the manuscript and according have a discussion on this issue in later

21 section.

3. Results and discussion

3.1 Estimated traffic activity and vehicle emissions

25   Table 3 presents spatially-explicit traffic counts during a typical weekday and an evening rush hour

26 (i.e., 6 p.m.), respectively. More than 80% of total daily traffic counts were concentrated in the MP, 160%

27 higher than the overall average of Macao. In particular, the Saint Antony Parish with internationally-

28 renowned tourist attraction (e.g., the Ruins of St. Paul's) had a top hour-based density of daily traffic

29 volume as a result of its substantial population density. Furthermore, traffic activity (unit veh km h^{-1} or

30 veh km d^{-1}) can be estimated as the product of traffic counts and link length, namely $TV_{h,l,v}$ and L_l (see

1   Equation 1), which is an essential indicator of vehicle-use intensity. Estimated daily traffic activity of

2   Macao's total vehicles in a typical weekday of 2010 is 4.04×10^6 veh km d^{-1} (see Table S1). LDPVs and

3   MCs rank first and second among all vehicle classifications, accounting for 43% and 30% of total daily

4   traffic activity in Macao. Therefore, fleet-average daily vehicle kilometers travelled (VKT) of LDPVs and

5   MCs during weekdays of 2010 are 20.8 km and 11.7 km, respectively. If we ignore potential difference

6   between weekdays and weekends, fleet-average annual VKT of LDPVs and MCs registered in Macao are

7   7600 km and 4300 km as of 2010, which are quite comparable with our previous survey results. Those

8   values could be only responsible for traffic demand within Macao, considering a part of LDPVs travel

9   cross the boundary of the Macao SAR into Mainland China. It is worth noting that annual VKT of LDPVs

10   registered in Macao is significantly lower than those of Beijing and Guangzhou (Zhang et al., 2013 and

11   2014a). The major reason is the scale of Macao is much smaller than those megacities of Mainland China

12   (e.g., Beijing, Guangzhou), approximately 15 km from the northernmost parish in MP to the Coloane

13   Island. Since fewer MCs drive on the cross-sea bridges, a major part of MCs' traffic activity (note: in

14   particular for light-duty two-stroke MCs) is largely limited within MP or TCC. Therefore, traffic activity

15   of MCs is lower than LDPVs although with higher traffic counts, whose estimated annual VKT is

16   comparable to the value in Mainland China (e.g., 5000~6000 km) (Zhang et al., 2013 and 2014a).

17   Table 4 presents estimated average distance-specific emission factors of major air pollutants by

18   vehicle classification and fuel type for that typical weekday in Macao during 2010. Average CO and THC

19   emission factors for gasoline powered LDPVs in Macao are significantly lower by 57% and 30%,

20   respectively, compared to those of gasoline LDPVs registered in Beijing, although the average driving

21   speed of LDPVs in Macao is lower than Beijing (e.g., ~22 km h^{-1} vs. 30 km h^{-1}). A major reason for that

22   estimation is a majority of the gasoline cars are imported from Japan, where vehicle emission standards

23   are in general more stringent than those implemented in Mainland China (Wang et al., 2014). By contrast,

24   compared to gasoline taxis in Beijing, diesel engines applied in the taxi fleet in Macao led to significantly

25   higher NO_X and $PM_{2.5}$ emission factors by 3.5 times and 17 times (Hu et al., 2012; Zhang et al., 2014a).

26   For heavy-duty trucks and buses, lower speed and a higher proportion of older vehicles result in higher

27   NO_X and $PM_{2.5}$ emission factors for those heavy-duty diesel vehicles in Macao than those in Beijing. For

28   MCs, in particular light-duty two-stroke MCs, their fleet-average THC emission factors are significantly

29   higher than other vehicle technology types (Zhou et al., 2014).

30   Estimated total vehicular emissions in a typical weekday during 2010 are 16.8 tons of CO, 3.58 tons

31   of THC, 5.00 tons of NO_X and 0.28 tons of $PM_{2.5}$. As Fig. 4 illustrates, emission allocation patterns by

1   vehicle classification are different for various pollutant categories. Compared to well-controlled CO and

2   THC emission factors of LDPVs, MCs are estimated to have been responsible for 69% and 72% of total

3   vehicular emissions for CO and THC respectively. In particular, two-stroke MCs contribute 45% of total

4   THC vehicular emissions, which led Macao government to initiate a replacement of two-stroke MCs with

5   small-size four-stroke MCs after 2010. Further, a possible promotion of electric MCs in Macao is also

6   under consideration by policy-makers in Macao. For both NO_X and $PM_{2.5}$, diesel-powered passenger fleets

7   contributed 60~65% of total vehicular emissions, including PBs, taxis and HDPVs mainly owned by hotels

8   and casinos. By contrast, diesel trucks contributed approximately 15% to 20% of total NO_X and $PM_{2.5}$

9   emissions in Macao, substantially lower than the contribution of diesel trucks registered in other populated

10   cities of China (e.g., 30~35% for Beijing and Guangzhou) (Zhang et al., 2013 and 2014a). This

11   phenomenon should be attributed to the significantly higher passenger transportation demand than freight

12   transportation in Macao, as tourism and entertainment industry is the pillar of the local economy. Our

13   results clearly suggest policy-makers in Macao should carefully focus on various vehicle classifications

14   when facing emission mitigation targets for various air pollutants.

15   For CO_2 emissions, unfavorable operating conditions like lower driving speeds and frequent use of

16   air-conditioning systems resulted in substantial climate and energy penalties for passenger vehicles (e.g.,

17   LDPVs, taxis, PBs). For example, the estimated average CO_2 emission factor of LDPVs is 263 g km^{-1} (see

18   Table 4), a significant increase of approximately 25% compared to on-road measurement results under a

19   higher average speed (205~210 g km^{-1} at 30 km h^{-1}). This is equivalent to ~13 L per 100 km   fuel

20   consumption, indicating a substantial increase of CO_2 and fuel consumption under real-world driving

21   conditions than those measured under the type-approval conditions applied in current regulatory systems

22   (e.g., both Japan and Europe). Overall, the estimated total CO_2 emissions from all vehicle classifications

23   and all road links are 1001 tons during a typical day. LDPVs, PBs and taxis are estimated to have been

24   responsible for 46%, 14% and 12% of total daily CO_2 emissions, respectively (see Fig. 4), ranking in the

25   top three among all classifications.

26   Our previous evaluation indicates estimated macro uncertainty (i.e., annual emission inventory by

27   using registration data) for air pollutants (e.g., CO, THC, NO_X and $PM_{2.5}$) is approximately -30%/+50%

28   at a 95% confidence level (Zhang et al., 2014a). The skewed probability distribution is due to high emitters

29   of air pollutants within the fleet. The uncertainty in CO_2 emissions would be narrower due to detailed

30   localized vehicle information and fuel economy data are used in estimation, plus it is strongly corrected

31   by average speed. It is noted that the Macao SAR is a relatively closed island city with special broader

controls (e.g., road transport to Mainland China). Only the vehicles issued with special license plates in the Macao SAR and Guangdong province (i.e., two license plates) can be driven across the border. This circumstance offers an opportunity to validate the gasoline fuel CO_2 emissions with the statistical fuel consumption record, since almost all the gasoline fuels are consumed by on-road vehicles in Macao. Our emission inventory estimated that total gasoline consumption by on-road vehicles in Macao would be 180 t during a typical weekday of 2010 (note: the carbon mass fraction is assumed 0.87). If using this value as the daily average through 365 days in a year, total gasoline consumption would be 65.7 kt in 2010, compared to a statistical consumption amount of 81.7 thousand m^3 (approximately 60 kt). The relative bias is within a reasonably narrow range (~10%) and can be attributed to two major reasons. First, the yearly estimation of gasoline consumption (65.7 kt) assumed the same vehicle activity on weekdays and weekends. The vehicle activity on weekends might be probably less than that on weekdays due to the absent commuting demand. Second, the gasoline price in Guangdong province was lower by approximately 20% than Macao during 2010, which could be an important incentive for the users of those LDPVs with two license plates to choose refilling their vehicles in Guangdong while using in Macao. For the diesel sector, the statistical data don't specify the amount consumed by on-road vehicles, and non-road engines would contribute substantially to the total diesel use in Macao. We suggest further validation be conducted if the on-road diesel consumption amount is available, since diesel vehicles could considerably account for total NO_X and $PM_{2.5}$ emission even their traffic fractions are at a low level (Dallmann et al., 2013). We could address the uncertainty in link-level vehicle emissions with the traffic big data (see the discussion in the next sub-section) available for typical roads in the future.

3.2 Temporal and spatial variations in traffic-related emissions

High strong correlations between temporal variations in traffic activity and emissions are clearly observed for all air pollutants and CO_2 (R^2>0.92, see Fig. 5). For example, the 6 p.m. hour contributed 6.9% of total daily traffic activity, when hourly emissions of gaseous species (CO, THC, NO_X and CO_2) were responsible for 7.9%~8.7% of their daily emissions. This was because emission factors of gaseous pollutants and CO_2 were increased during the rush hours due to lower driving speed. The increases were 15%~26% for their emission factors compared to the daily averages. Compared with the night time, average gaseous emission factors of the total fleet were increased by 51%~120%. The elevation of $PM_{2.5}$ emissions in the rush hour was not as significant as gaseous species, because the traffic demand of diesel

1 fleets (e.g., HDPVs, taxis, PBs, trucks) was increased less relative to gasoline fleets (e.g., MCs, LDPVs)

2 in Macao.

3   Spatial distributions of vehicular emissions are associated with real-world traffic characteristics

4 including total traffic counts, traffic conditions and fleet composition. To sum up, 58% of NO_X, 52% of

5 $PM_{2.5}$ and 59% of CO_2 vehicular emissions were estimated from the road network of the MP (see Fig. 6

6 for NO_X, Fig. S8 for other pollutants and Table S2 for the summary of spatial distribution). Meanwhile,

7 76% of CO and 78% of THC emissions were aggregated from on-road vehicles within the MP. The

8 discrepancy of emission spatial allocations between CO/THC and NO_X/$PM_{2.5}$/CO_2 is primarily because

9 the higher fleet penetration of MCs in the MP. That is to say, relative inaccuracy associated with emission

10 spatial allocation by the top-down approach could be up to 20% if real-world fleet composition

11 information is not taken into account. By contrast, the spatial allocations of NO_X, $PM_{2.5}$ and CO_2 at three

12 cross-sea bridges were estimated to be higher by approximately 55~110% than CO and THC, because the

13 traffic volume fraction of MCs was significantly lower than in other regions, in particular compared with

14 the MP.

15   Detailed statistical profiles of spatial-related vehicular emission are summarized by length-specific

16 emission intensity of road groups and area-specific emission intensity of gridded cells (see Table 5 and

17 Table 6). Higher length-specific emission intensities of CO and THC are unexpectedly identified on

18 arterial roads in the MP with less traffic accounts compared with their urban freeway counterparts, owing

19 to higher traffic activity of MCs and more severe traffic congestion increasing all-fleet emission factors.

20 For NO_X, $PM_{2.5}$ and CO_2, higher length-specific emission intensities are all associated with higher level

21 of service for the three road classes, both in the MP and the TCC. Area-specific emission intensities of all

22 pollutants and CO_2 had decreasing trends from north to south (i.e., from the MP to the Coloane Island),

23 similar to the patterns of road density and traffic demand. Emission hotspots are identified in traffic-

24 populated cells of the MP, e.g., the region close the Ruins of St. Paul's, where daily area-specific emission

25 intensity of NO_X was as high as 600 kg km^{-2} d^{-1}. This level is ~4 times of that in the entire Macao and ~40

26 times of the Coloane Island. Not surprisingly, significant near-field air pollution problems in MP are

27 caused by those extremely higher vehicular emissions due to higher traffic activity density and more

28 significant traffic congestion.

29   It should be noted that increasingly broad application of an intelligent traffic system (ITS) and smart

30 vehicle technologies can play a significant role in improving our understanding of dynamic traffic flows,

31 namely enabling the big data collection regarding total traffic volume, fleet composition and traffic

conditions (e.g., speed). For example, the traffic loop detector (TLD) and the vehicle license plate recognition (VLPR) are both widely-used and economic ITS technologies that began in the early 2000s in China and are integrated to provide category-informed vehicle volume, on which many cities in China (e.g., Beijing, Guangzhou) depend to release official data including year-by-year variations in total urban traffic demand (BJTRC, 2013; Zhang et al., 2013). The traffic loop detector is able to provide vehicle passing speed, however, which is often criticized due to the limited coverage for the entire trips or entire traffic network. The floating car system, namely using the taxi fleet as probe vehicles based on GPS technology, is an advanced monitoring tool for real-time traffic conditions. Taking Beijing for example, its floating car system is capable of mapping link-based traffic conditions for the urban area (~1000 km^2) every five minutes based on 66 thousand taxis and mesh urban average speed layer down at a link level. During 2012, 24-h average speeds of the urban area of Beijing were estimated at 23.2 ± 2.3 km h^{-1} for weekdays and 26.9 ± 3.9 km h^{-1} for weekends and holidays, respectively (BJTRC, 2014; Zhang et al., 2014a and 2014b). Therefore, daily variations in traffic conditions could result in a coefficient of variation (i.e., the ratio of standard deviation to mean value) of 6% for the distance-specific CO_2 emission factor all year around in Beijing. The speed correction applied for this variation estimation is also applicable to the Macao's road network. If the evaluation level is refined into a link-level, the variability and uncertainty in vehicle emissions would be greater due to traffic flows became inherently greater as the spatial resolution was enhanced. For example, the variations in hourly speeds of arterial roads in the MP could led to variations (e.g., one standard deviation, namely 40% in the noon time and 48% in the rush hours) in fleet-average CO_2 emission factors of gasoline LDPVs of approximately -20% to 45% during the noon time and -25% to 60% during rush hours relative to the average CO_2 emission factor levels. In terms of total vehicle emissions, it would be further complicated since the traffic volume is inherently associated with the level of service (e.g., speed) in reality. Most recently, the radio frequently identification (RFID) technology has been applied in a few Chinese cities (e.g., Nanjing, the capital city of Jiangsu province) to provide more accurate vehicle recognition with detailed specifications (e.g., category, fuel type, emission standard, model year, and vehicle size) than the TLD and the VLPR. The RFID data in Nanjing are further connected with a smartphone application, based on which more capabilities like environmentally-constrained traffic management (e.g., low emission zone, congestion fee program) could be developed in the future. From the perspective of vehicles, for instance, more real vehicle data can be accessed through the on-board diagnostic (OBD) decoders. The second-by-second data of driving conditions (e.g., speed, acceleration) are able to be combined with operating mode-based (e.g., VSP-informed) emission model

1   to provide finer emission estimations. While foregoing advanced traffic data collection methods (e.g.,

2   TLD, RFID, taxi fleet based floating car system) are not available in Macao, the framework of this study

3   is technically feasible to large cities in China when the traffic big data are adequately available.

5   **3.3 Simulated concentrations of primary traffic-related pollutants in Macao**

6   Fig. 7 presents a spatial map of average concentrations of primary vehicle-contributed CO (see $PM_{2.5}$

7   in Fig. S9), which shows the simulated results of all receptors (i.e., central points of cells) with the

8   AERMOD model. The spatial variations in simulated concentrations highly resemble the patterns of area-

9   specific emission intensity for vehicular pollutants. For example, average concentrations contributed by

10   local vehicular emissions in Macao were 86.1 ± 89.4 μg m^{-3} of CO and 1.30 ± 0.91 μg m^{-3} of $PM_{2.5}$,

11   respectively (see Table 7). Highest receptor concentrations of CO and $PM_{2.5}$ are 415 and 4.42 μg m^{-3},

12   respectively, all occurring at traffic-populated cells in the MP.

13   We further compared modeled concentrations of primary pollutants from local vehicles and official

14   air quality data. Traffic contributions at the monitoring sites are approximated by simulated results for

15   their closest receptors as to estimate monthly-average source proportions of on-road vehicles in Macao.

16   Therefore, source proportions vary from pollutant categories and locations during the time framework of

17   this study. For example, estimated proportions of vehicular CO emissions are ~25-30% in the MP and

18   ~15% in the Taipa Island, indicating lower impacts compared to regional contributions. With regard to

19   $PM_{2.5}$, estimated proportions of primary vehicular $PM_{2.5}$ emissions are minor, since the atmospheric

20   secondary $PM_{2.5}$ considerably contributed by vehicle emissions is not considered in this study, which need

21   to be applied with a very detailed regional emission inventory including all anthropogenic emission

22   sources and complex air quality models with sophisticated source apportionment functions. This is beyond

23   the scope of this paper. We acknowledge two aspects of uncertainty regarding the AERMOD simulation.

24   First, the strong street-canyon effects in the building-dense MP which are not sophisticatedly addressed

25   by the AERMOD. Tang and Wang (2007) coupled the OSPM model and detailed building-based

26   geography layer to simulate CO concentrations in the MP under assumed traffic scenarios to address the

27   street canyon effect. Second, the setup of 500 m×500 m cells used in the AERMOD simulation is not

28   adequate to present the concentration gradients near major roads and the fine air pollution hotspots. For

29   hotspots, advanced computational fluid dynamics (CFD)-based micro-scale air quality model coupled

30   with sophisticated gaseous chemical mechanisms and aerosol dynamics are suggested to quantitatively

assess potential impacts and mitigation strategies from perspectives of traffic flows, weather conditions and architecture layout (Tong et al., 2011).

Usually, ambient NO_2 pollution in the urban area has strong associations with traffic emissions. In Macao, the ambient NO_2 concentration exceedance of the 40 μg m^{-3} level were seen in Macao. However, as we note in the methodology section, we don't include the NO_2 results in the manuscript due to major model limitations of AERMOD (e.g., instantaneous time framework of the basic reaction, inadequate spatial-resolved ambient ozone concentrations, and lacking considerations of other NO_X related chemical reactions). If the Community Multiscale Air Quality (CMAQ) model, a regional scale air quality model including regional transport and sophisticated chemical mechanisms, is applied to address these issues, the simulated NO_2 results by using CMAQ would be significantly lower than observed concentrations (see Supplementary Information). Moreover, although a fine grid setup with a 4 km × 4 km resolution is used over Macao, only 6 cells would be created in Macao (note: 4 cells shared by Macao and Zhuhai together, a city in Mainland China and adjacent to Macao). Thereby, advanced air quality simulation technology with finer spatial resolution is required to make the use of this link-level emission inventory, since the urban air quality and health impact issues could be very spatially heterogeneous because of the land use policy and the topology of traffic network.

4. Conclusions

High-resolution vehicle emission inventory is a valuable assessment tool to achieve the fine air quality administration, in particular for traffic-populated East Asian cities where traffic management is an essential approach to reduce emissions. Due to the difficulties in obtaining link-level traffic flow data and localized emission measurement profiles, such a dedicated environmental tool has not been developed at the link-level which covers a whole city and all vehicle categories. This study selected the entire area of Macao, the most populated city in this world, to demonstrate a high-resolution simulation of vehicular pollution by coupling detailed local data collected and inter-disciplinary models (e.g., traffic demand).

Our traffic flow investigation and simulation results showed that total daily traffic activity during a typical weekday of 2010 was estimated at 4.06 million veh km d^{-1}. Passenger trips using MCs, LDPVs, taxis and buses were responsible for a dominant part of travel demand in Macao, accompanied by a smaller traffic fraction of on-road freight transportation (e.g., trucks) than other cities in Mainland China. Spatial heterogeneity of traffic flow characteristics has been discerned between the MP and the remaining parts (i.e., the TCC) of Macao. For example, the MP contributed over 80% of total traffic accounts in Macao

1   during a weekday of 2010 and MCs were more prevalent in this more populated peninsula compared to

2   the TCC. Tremendous travel demand created during rush hours resulted in significant traffic congestion,

3   indicated by an average speed lower than 15 km h^{-1} for arterial and residential roads in the MP.

4   Based on a localized vehicle emission model (e.g., the EMBEV-Macao) and high-resolution traffic

5   profiles regarding traffic volume, average speed and fleet composition, this study established a link-based

6   vehicle emission inventory with high resolution meshed in a temporal and spatial framework (e.g., hourly

7   and link-level). We estimated that total daily vehicle emissions in Macao were 16.6 tons of CO, 3.58 tons

8   of THC, 5.00 tons of NO$_X$, 0.28 tons of PM$_{2.5}$ and 1001 tons of CO$_2$ during a typical weekday of 2010.

9   The gasoline fuel CO$_2$ emissions based on the link-level inventory were in a good agreement with the

10 statistical gasoline consumption record in Macao. MCs are the major contributor to CO and THC

11 emissions due to their higher emission factors than LDPVs. Diesel-powered passenger fleets like buses

12 and taxis contributed 60~65% of total vehicular emissions of NO$_X$ and PM$_{2.5}$. With a special focus on the

13 MP region, where traffic density and congestion are more significant, area-specific emission intensity can

14 be higher than the average of the entire Macao area by 135% for CO, 145% for THC, 85% for NO$_X$, 65%

15 for PM$_{2.5}$ and 90% for CO$_2$. The geographic discrepancy of spatial allocation between THC and PM$_{2.5}$

16 emissions can be attributed to the spatially heterogeneous vehicle-use intensity between MCs and diesel

17 fleets (e.g., higher use intensity of MCs in the MP); and this trait could not be identified by using the

18 traditional emission inventory tool. From the perspective of temporal variations, hourly emissions of CO,

19 THC, NO$_X$ and CO$_2$ during the evening traffic peak could be responsible for 7.9%~8.7% of total daily

20 emissions, when their emission factors were increased by 15%~26% compared to the daily averages due

21 to the traffic congestion.

22   We further employed the AERMOD model to quantify average concentrations of CO and PM$_{2.5}$

23 contributed by primary vehicle emissions in Macao. Our simulation indicated receptor-averaged

24 concentrations from primary vehicle emissions were 84.5 ± 86.1 μg m^{-3} of CO and 1.30 ± 0.91 μg m^{-3} of

25 PM$_{2.5}$, respectively, during the weekdays of November, 2010. The highest receptor concentrations of CO,

26 NO$_X$ and PM$_{2.5}$ were 415 μg m^{-3} and 4.42 μg m^{-3}, respectively, all occurring at traffic-populated cells in

27 the MP. Advanced air quality simulation technology with higher spatial resolution and sophisticated

28 chemical transport mechanisms is required to make the use of the link-level emission inventory and better

29 address local air quality issues (e.g., NO$_2$ pollution). This paper can provide a useful case study and a solid

30 framework for developing high-resolution environmental assessment tools for other vehicle-populated

31 cities in the world. We also highlighted the importance of real traffic data using ITS techniques and the

traffic big data approaches to future high-resolution simulation for larger cities in the East Asia and all over the world.

Acknowledgments. This work was sponsored by the National High Technology Research and Development Program (863) of China (No. 2013AA065303), the National Natural Science Foundation of China (No. 91544222), and the Program for New Century Excellent Talents in University (NCET-13-0332) . We thank Miss Xiao Fu of Tsinghua University for her help in running the CMAQ Model. The contents of this paper are solely the responsibility of the authors and do not necessarily represent official views of the sponsors.

References

Benbrahim-Tallaa, L, Baan, R.A., Grosse, Y., Lauby-Secretan, B., Ghissassi, F.E., Bouvard, V., Guha, N., Loomis, D., Straif, K.: Carcinogenicity of diesel-engine and gasoline-engine exhausts and some nitroarenes. Lancet Oncol., 13(7), 663-664, 2012

Beijing Transport Research Center: Beijing Transportation Annual Report 2013. 2014 (accessed), available at: www.bjtrc.org.cn

Bishop, G.A., Schuchmann, B.G., Stedman, D.H., Lawson, D.R.: Multispecies remote sensing measurements of vehicle emissions on Sherman Way in Van Nuys, California. J. Air Waste Manage. Assoc., 62, 1127-1133, 2012

Carslaw, D.C., Beevers, S.D., Tate, J.E., Westmoreland, E.J., Williams, M.L.: Recent evidence concerning higher NOx emissions from passenger cars and light duty vehicles. Atmos. Environ., 45(39), 7053-7063, 2011.

Carslaw, D.C., Rhys-Tyler, G.: New insights from comprehensive on-road measurements of NO_X, NO_2 and NH_3 from vehicle emission remote sensing in London, UK. Atmos. Environ., 81, 339-347, 2013.

Chen, Y., Borken-Kleefeld, J.: Real-driving emissions from cars and light commercial vehicles – Results from 13 years remote sensing at Zurich/CH. Atmos. Environ., 88, 157-164, 2014.

Chen, Y., Borken-Kleefeld, J.: New emission deterioration rates for gasoline cars – Results from long-term measurements. Atmos. Environ., 101, 58-64, 2015.

Department of Statistics and Census Service (DSEC), Macao: Statistical Information System of Macao. 2014 (accessed). Available at http://www.dsec.gov.mo/default.aspx

Dallmann, T.R., Kirchstetter, T.W., DeMartini, S.J., Harley, R.A.: Quantifying on-road emissions from gasoline-powered motor vehicles: Accounting for the presence of medium- and heavy-duty diesel trucks. Environ. Sci. Techno., 47(23), 13873-13881, 2013.

Du, X., Wu, Y., Fu, L. Wang, S., Zhang, S., Hao, J.: Intake fraction of $PM_{2.5}$ and NO_X from vehicle emissions in Beijing based on personal exposure data. Atmos. Environ., 57, 233-243, 2012.

EEA (European Environmental Agency): European Union emission inventory report 1990–2012 under the UNECE Convention on Long-range Transboundary Air Pollution (LRTAP). Annex I_European Union (EU-27) LRTAP emission data. 2014. Available at http://www.eea.europa.eu/publications/lrtap-2014

Franco, V., Sánchez, F.P., German, J., Mock, P.: Real-world exhaust emissions from modern diesel cars. The International Council on Clean Transportation Report, 2014. Available at http://www.theicct.org/real-world-exhaust-emissions-modern-diesel-cars

Goh, M.: Congestion management and electronic road pricing in Singapore. J. Transp. Geogr., 10(1), 29-38, 2002.

HKCSD (Hong Kong Census and Statistics Department): Hong Kong Statistics, 2014. Available at http://www.censtatd.gov.hk/hkstat/index.jsp

Holmes, N.S., Morawska, L.: A review of dispersion modelling and its application to the dispersion of particles: An overview of different dispersion models available. Atmos. Environ., 40(30), 5902-5928, 2006

Hu, J., Wu, Y., Wang, Z., Li, Z., Zhou, Y., Wang, H., Bao, X., Hao, J.: Real-world fuel efficiency and exhaust emissions of light-duty diesel vehicles and their correlation with road conditions. J. Environ. Sci., 24(5), 865-874, 2012.

Huo, H., Zhang, Q., He, K., Wang, Q., Yao, Z., Streets, D.: High-resolution vehicular emission inventory using a link-based method: a case study of light-duty vehicles in Beijing. Environ. Sci. Techno., 43(7), 2394-2399.

Ji, S., Cherry, C.R., Bechle, M.J., Wu, Y., Marshall, J.D.: Electric vehicles in China: emissions and health impacts. Environ. Sci. Techno., 46(4), 2018-2024, 2012.

Lee, T., Frey, F.: Evaluation of representativeness of site-specific fuel-based vehicle emission factors for route average emissions. Environ. Sci. Techno., 46(12), 6867-6873

MEP (Ministry of Environmental Protection, P. R. China): Bulletin of China's Environmental Status in 2013. 2014. Available at http://jcs.mep.gov.cn/hjzl/zkgb/2013zkgb (in Chinese)

Misra, A., Roorda, M.J., MacLean, H.L.: An integrated modelling approach to estimate urban traffic emissions. Atmos. Environ., 73, 81-91: 2013

McDonald, B.C., McBride, Z.C., Martin, E.W., Harley, R.A.: High-resolution mapping of motor

Murphy, J.G., Day, D.A., Cleary, P.A., Wooldridge, P.J., Millet, D.B., Goldstein, A.H., Cohen, R.C.: The weekend effect within and downwind of Sacramento – Part 1: Observations of ozone, nitrogen oxides and VOC reactivity. Atmos. Chem. Phys., 7, 5327-5339, 2007.

NBSC (National Bureau of Statistics of China): China Statistical Yearbook, 2014.

Podrez, M.: An update to the ambient ratio method for 1-h NO2 air quality standards dispersion modeling. Atmos. Environ., 103, 163-170, 2015.

Pollack, I.B., Ryerson, T.B., Trainer, M., Parrish, D.D., Andrews, A.E., Atlas, E.L., Blake, D.B., Brown, S.S., Commane, R., Daube, B.C., de Gouw, J.A., Dubé, W.P., Flynn, J., Frost, G.J., Gilman, J.B., Grossberg, N., Holloway, J.S., Kofler, J., Kort, E.A., Kuster, W.C., Lang, P.M., Lefer, B., Lueb, R.A., Neuman, J.A., Nowak, J.B., Novelli, P.C., Peischl, J., Perring, A.E., Roberts, J.M., Santoni, G., Schwarz, J.P., Spackman, J.R., Wagner, N.L., Warneke, C., Washenfelder, R.A., Wofsy, S.C., Xiang, B.: Airborne and ground-based observations of a weekend effect in ozone, precursors, and oxidation products in the California South Coast Air Basin. J. Geography. Res. Atmos., 117, D00V05, 2012.

Saikawa, E., Kurokawa, J., Takigawa, M., Borken-Kleefeld, J., MauzeralL, D.L., Horowitz, L.W., Ohara, T.: The impact of China's vehicle emissions on regional air quality in 2000 and 2020: a scenario analysis. Atmos. Chem. Phys., 11, 9465-9484, 2011.

Shindell, D., Faluvegi, G., Walsh, M., Anenberg, S.C., van Dingenen, R., Muller, N.Z., Austin, J., Koch, D., Milly, G.: Climate, health, agricultural and economic impacts of tight vehicle-emission standards. Nature Climate Change, 1, 59-66, 2011.

Sheng, N., Tang, U.W.: A building-based data capture and data mining technique for air quality assessment. Front. Environ. Sci. Engin. China, 5(4), 543-551, 2011.

Tang, U.W., Wang, Z.: Influences of urban forms on traffic-induced noise and air pollution: Results from a modelling system. Environ. Model. Softw., 22(12), 1750–1764, 2007.

Tong, Z., Wang, Y.J., Patel, M., Kinney, P., Chrillrud, S., Zhang, K.M.: Modeling spatial variations of black carbon particles in an urban highway-building environment. Environ. Sci. Techno., 46(1), 312-319, 2011.

Transportation Bureau of Macao (TBM: Consultation report on the road transportation policy planning of Macao 2010-2020. 2010. Available at http://www.dsat.gov.mo/ptt/sc/doc.pdf

Transport for London: London Atmospheric Emissions Inventory 2010, Methodology Document. 2014 (assessed), available at http://data.london.gov.uk/dataset/london-atmospheric-emissions-inventory-2010

Uherek, E., Halenka, T., Borken-kleefeld, J., Balkanski, Y., Bernstsen, T., Borrego, C., Gauss, M., Hoor, P., Juda-Rezler, K., Lelieveld, J., Melas, D., Rypdal, K., Schmid, S.: Transport impacts on atmosphere and climate: Land transport. Atmos. Environ., 44(37), 4772-4816, 2010.

U.S. EPA (U.S. Environmental Protection Agency): AERMOD: Description of model formulation, 2004. Available at http://www.epa.gov/scram001/7thconf/aermod/aermod_mfd.pdf

U.S. EPA: The 2011 National Emissions Inventory (NEI), 2014 (accessed). Available at http://www.epa.gov/ttn/chief/net/2011inventory.html

U.S. EPA: Technical support document (TSD) for NO2-related AERMOD modifications, 2015. Available at https://www3.epa.gov/scram001/11thmodconf/AERMOD_NO2_changes_TSD.pdf

Velders, G. J. M., Geilenkirchen, G. P., Lange, R. d.: Higher than expected NO_X emission from trucks may affect attainability of NO_2 limit values in the Netherlands. Atmos. Environ., 45, 3025-3033, 2011.

Vestreng, V., Ntziachristos, L., Semb, A., Reis, S., Isaksen, I.S.A., Tarrasón, L.: Evolution of NOx emissions in Europe with focus on road transport control measures. Atmos. Chem. Phys., 9, 1503-1530, 2009.

Vallamsundar, S., Lin, J.: MOVES and AERMOD used for $PM_{2.5}$ conformity hot spot air quality modeling. J. Trans. Res. Board, 2270, 39-48, 2012.

Walsh, M.P.: $PM_{2.5}$: global progress in controlling the motor vehicle contribution. Front. Environ. Sci. En., 8(1), 1-17, 2014.

Wang, H., Fu, L., Lin, X., Zhou, Y., Chen, J.: A bottom-up methodology to estimate vehicle emissions for the Beijing urban area. Sci. Total Environ., 407(6), 1947-1953, 2009

Wang, X., Westerdahl, D., Wu, Y., Pan, X., Zhang, K.M.: On-road emission factor distributions of individual diesel vehicles in and around Beijing, China. Atmos. Environ., 45(2), 503-513, 2011.

Wang, X., Westerdahl, D., Hu, J., Wu, Y., Yin, H., Pan, X., Zhang, K. M.: On-road diesel vehicle emission factors for nitrogen oxides and black carbon in two Chinese cities. Atmos. Environ., 46, 45-55, 2012a.

Wang, Z., Wu, Y., Zhou, Y., Li, Z., Wang, Y., Zhang, S., Hao, J.: Real-world emissions of gasoline passenger cars in Macao and their correlation with driving conditions. Int. J. Environ. Sci. Techno., 11(4), 1135-1146, 2014

Wu, Y., Wang, R., Zhou, Y., Lin, B., Fu, L., He, K., Hao, J.: On-Road vehicle emission control in Beijing: past, present, and future. Environ. Sci. Technol., 45(1), 147–153, 2011.

Wu, X., Zhang, S., Wu, Y., Un, P., Ke, W., Fu, L., Hao, J.: On-road measurement of gaseous emissions and fuel consumption for two hybrid electric vehicles in Macao. Atmos. Pollu. Res., 6, 858-866, 2015.

Wu, X., Zhang, S., Wu, Y., Li, Z., Fu, L., Hao, J.: Real-World Emissions and Fuel Consumption of Diesel Buses and Trucks in Macao: From On-road Measurement to Policy Implications. Atmos. Environ., 120, 393-403, 2015.

Zannetti, P.: Air Pollution Modeling. Springer US, 1990.

Zhang, S., Wu, Y., Liu, H., Wu, X., Zhou, Y., Yao, Z., Fu, L., He, K., Hao, J.: Historical evaluation of vehicle emission control in Guangzhou Based on a multi-year emission inventory. Atmos. Environ., 76, 32-42, 2013.

Zhang, S., Wu, Y., Wu, X., Li, M., Ge, Y., Liang, B., Xu, Y., Zhou, Y., Liu, H., Fu, L., Hao, J.: Historic and future trends of vehicle emissions in Beijing, 1998–2020: A policy assessment for the most stringent vehicle emission control program in China. Atmos. Environ., 89, 216-219, 2014a.

Zhang, S., Wu, Y., Liu, H., Huang, R., Un, P., Zhou, Y., Fu, L., Hao, J.: Real-world fuel consumption and CO_2 (carbon dioxide) emissions by driving conditions for light-duty passenger vehicles in China. Energy, 69, 247-257, 2014b.

Zhang, S., Wu, Y., Liu, H., Huang, R., Yang, L., Li, Z., Fu, L., Hao, J.: Real-world fuel consumption and CO2 emissions of urban public buses in Beijing. Applied Energy, 113, 1645-1655, 2014c

Zhang, S., Wu, Y., Hu, J, Huang, R., Zhou, Y., Bao, X., Fu, L., Hao, J.: Can Euro V heavy-duty diesel engines, diesel hybrid and alternative fuel technologies mitigate NOx emissions? New evidence from on-road tests of buses in China. Appl. Energy, 132, 118-126, 2014d

Zheng, B., Huo, H., Zhang, Q., Yao, Z.L., Wang, X.T., Yang, X.F., Liu, H., He, K.B.: High-resolution mapping of vehicle emissions in China in 2008. Atmos. Chem. Phys., 14, 9787-9805, 2014

Zheng, X., Wu, Y., Jiang, J., Zhang, S., Liu, H., Song, S., Li, Z., Fan, X., Fu, L., Hao, J.: Characteristics of on-road diesel vehicles: Black carbon emissions in Chinese cities based on portable emissions measurement. Environ. Sci. Techno., accepted, 2015

Zhou, Y., Wu, Y., Yang, L., Fu, L., He, K., Wang, S., Hao, J., Chen, J., Li, C.: The impact of transportation control measures on emission reductions during the 2008 Olympic Games in Beijing, China. Atmos. Environ., 44, 285-293, 2010.

Zhou, Y., Wu, Y., Zhang, S., Fu, L., Hao, J.: Evaluating the emission status of light-duty gasoline vehicles and motorcycles in Macao with real-world remote sensing measurement. J. Environ. Sci., 26(11): 2240-2248, 2014.

1   Tables

3   **Table 1.** 24-h allocations of total traffic counts by region and road class during weekdays in Macao, 2010

Region	The Macao Peninsula			The Taipa-CoTai-Coloane Region		
Road classes	Freeway	Arterial	Residential	Freeway	Arterial	Residential
0	0.021	0.017	0.021	0.021	0.017	0.022
1	0.013	0.014	0.013	0.013	0.014	0.013
2	0.011	0.009	0.011	0.011	0.010	0.011
3	0.009	0.007	0.009	0.009	0.007	0.009
4	0.008	0.007	0.008	0.008	0.007	0.008
5	0.008	0.008	0.008	0.008	0.008	0.008
6	0.021	0.024	0.020	0.021	0.024	0.021
7	0.029	0.051	0.029	0.029	0.022	0.030
8	0.051	0.057	0.059	0.048	0.053	0.061
9	0.048	0.054	0.048	0.042	0.052	0.051
10	0.044	0.049	0.050	0.046	0.055	0.049
11	0.055	0.050	0.049	0.056	0.056	0.048
Hour 12	0.051	0.056	0.055	0.051	0.056	0.058
13	0.059	0.062	0.061	0.062	0.064	0.062
14	0.060	0.066	0.064	0.070	0.073	0.059
15	0.064	0.061	0.059	0.068	0.072	0.065
16	0.066	0.061	0.060	0.071	0.070	0.046
17	0.066	0.066	0.059	0.065	0.069	0.069
18	0.071	0.066	0.076	0.062	0.060	0.070
19	0.061	0.057	0.062	0.054	0.051	0.075
20	0.049	0.045	0.052	0.049	0.046	0.045
21	0.048	0.041	0.052	0.048	0.042	0.050
22	0.047	0.039	0.042	0.047	0.039	0.039
23	0.042	0.033	0.032	0.042	0.034	0.033

Table 2. Summary of age allocation for on-road fleets by vehicle classification in Macao

Vehicle classification		LDPV		MC		Taxi	PB		MDPV		HDPV	LDT		HDT
Sub-classification		G [a]	D [b]	Heavy [c]	Light [c]	D	Medium [d]	Heavy [d]	G	D	D	G	D	D
Ratio		0.99	0.01	0.68	0.32	1.00	0.33	0.67	0.53	0.47	1.00	0.25	0.75	1.00
	1	0.12	0.12	0.18	0.09	0.14	0.00	0.08	0.20	0.16	0.20	0.12	0.08	0.02
	2	0.10	0.17	0.15	0.08	0.13	0.00	0.08	0.17	0.17	0.06	0.17	0.18	0.15
	3	0.10	0.08	0.19	0.09	0.04	0.00	0.08	0.07	0.12	0.09	0.11	0.10	0.11
	4	0.10	0.11	0.14	0.07	0.06	0.00	0.18	0.06	0.02	0.10	0.03	0.09	0.04
	5	0.09	0.03	0.08	0.04	0.06	0.17	0.16	0.05	0.09	0.09	0.03	0.05	0.03
	6	0.06	0.05	0.05	0.07	0.02	0.12	0.14	0.05	0.03	0.09	0.09	0.04	0.01
	7	0.05	0.01	0.04	0.04	0.11	0.25	0.15	0.06	0.01	0.03	0.00	0.02	0.01
	8	0.05	0.02	0.04	0.07	0.16	0.05	0.05	0.08	0.01	0.05	0.05	0.02	0.00
	9	0.04	0.03	0.02	0.08	0.24	0.00	0.00	0.04	0.01	0.05	0.02	0.02	0.01
Vehicle age	10	0.04	0.06	0.01	0.13	0.01	0.07	0.00	0.06	0.02	0.04	0.01	0.03	0.02
	11	0.05	0.06	0.03	0.14	0.03	0.17	0.01	0.02	0.01	0.10	0.02	0.04	0.01
	12	0.05	0.04	0.02	0.06	0.00	0.00	0.03	0.03	0.01	0.04	0.01	0.04	0.02
	13	0.03	0.06	0.00	0.01	0.00	0.03	0.00	0.02	0.03	0.00	0.02	0.02	0.01
	14	0.04	0.05	0.01	0.01	0.00	0.10	0.00	0.02	0.03	0.00	0.06	0.04	0.04
	15	0.03	0.05	0.01	0.01	0.00	0.05	0.00	0.04	0.05	0.00	0.06	0.04	0.11
	16	0.02	0.02	0.01	0.00	0.00	0.00	0.00	0.03	0.04	0.03	0.04	0.06	0.16
	17	0.01	0.03	0.00	0.01	0.00	0.00	0.00	0.00	0.03	0.00	0.05	0.04	0.06
	18	0.01	0.01	0.00	0.00	0.00	0.00	0.00	0.00	0.06	0.00	0.05	0.03	0.03
	19	0.00	0.00	0.00	0.00	0.00	0.00	0.04	0.00	0.02	0.00	0.02	0.02	0.07
	20	0.00	0.01	0.00	0.00	0.00	0.00	0.00	0.00	0.07	0.02	0.03	0.05	0.08
Fleet-average vehicle age		6.7	7.3	4.4	7.2	5.8	8.6	5.5	5.7	7.9	6.0	8.1	8.1	11.4

Note: [a] gasoline; [b] diesel; [c] breaking point of engine displacement 50 ml; [d] breaking point of engine displacement at 5.0 L.

1   **Table 3.** Spatially-explicit estimation of traffic counts in Macao

Region	Daily traffic counts by road class (10^5 veh)			Hour-based density of traffic volume (10^4 veh h^{-1} km^{-2})	
	Freeway	Arterial	Residential	Daily average	Evening rush hour (6 p.m.)
Macao Peninsula	15.2	70.8	138.4	10.0	17.3
Saint Antony Parish	2.8	20.5	35.0	25.3	44.3
Taipa-Cotai-Coloane	6.9	13.9	28.8	1.0	1.5
Taipa	2.2	12.5	17.8	2.0	3.1
Cotai	3.6	1.4	7.1	0.8	1.3
Coloane	1.1		3.9	0.3	0.5
Total	22.2	84.7	170.2	3.8	6.5

1   **Table 4.** Estimated fleet-average emission factors under real-world driving conditions

Vehicle classification	Fleet-average emission factors (g km^{-1})					Emission measurement data sources
	CO	THC	NO_X	$PM_{2.5}$	CO_2	
LDPV-Gasoline	1.74	0.34	0.28	0.006	263	PEMS [a], RS [b], EMBEV [c]
MDPV-Gasoline	2.80	1.78	1.03	0.030	379	RS
MDPV-Diesel	1.60	0.27	1.44	0.26	307	RS, EMBEV
HDPV-Diesel	4.76	0.25	10.9	0.48	914	RS, EMBEV
LDT-Gasoline	6.36	1.75	0.61	0.014	250	RS
LDT-Diesel	1.69	0.65	4.03	0.35	485	PEMS, RS, EMBEV
HDT-Diesel	7.40	0.94	12.3	0.95	1010	PEMS, RS, EMBEV
Taxi	0.47	0.06	0.86	0.11	192	PEMS, RS
MC-Light	7.95	4.07	0.26	0.030	39	RS
MC-Heavy	10.2	1.18	0.38	0.012	86	RS
PB-Medium	2.45	1.09	6.50	0.32	555	PEMS, RS, EMBEV
PB-Heavy	6.05	0.35	15.8	0.57	1215	PEMS, RS, EMBEV

2   Note: [a] PEMS measurement data in Macao; [b] Remote sensing data in Macao; [c]
3   Dynamometer or PEMS measurement data of sufficient vehicle samples involved in the
4   original EMBEV model (Zhang et al., 2014a).

1 **Table 5.** Length-specific emission intensity of total vehicular emissions during a typical
2 weekday of 2010

Region	Road class	Length-specific emission intensity ($kg\ km^{-1}\ d^{-1}$)				
		CO	THC	NO_X	$PM_{2.5}$	CO_2
Macao Peninsula	Freeway	141	28	43	2.6	9.05×10^3
	Arterial	195	42	39	1.9	7.82×10^3
	Residential	79	17	18	0.9	3.74×10^3
Taipa-Cotai-Coloane	Freeway	73	12	41	2.9	7.41×10^3
	Arterial	54	9	35	2.3	595×10^3
	Residential	24	5	6	0.4	1.91×10^3
Cross-sea bridges	Freeways	109	22	59	4.0	10.8×10^3
Total	Freeway	106	20	48	3.1	9.07×10^3
	Arterial	122	25	38	2.1	6.85×10^3
	Residential	59	13	14	0.7	3.08×10^3

4 **Table 6.** Area-specific emission intensity of total vehicular emissions during a typical
5 weekday of 2010

Region / Parish	Area-specific emission intensity ($kg\ km^{-2}\ d^{-1}$)				
	CO	THC	NO_X	$PM_{2.5}$	CO_2
Macao Peninsula	1368	297	312	15.5	6.37×10^4
St. Lazarus Parish	3118	681	695	33.7	12.9×10^4
St. Lawrence Parish	1407	303	305	15.4	6.13×10^4
Our Lady Fatima Parish	1241	271	274	13.7	5.74×10^4
St. Anthony Parish	2485	546	556	26.4	11.8×10^4
Cathedral Parish	784	166	199	10.4	3.86×10^4
Taipa	287	52	150	9.50	2.80×10^4
CoTai Reclamation Area	155	27	70	4.67	1.41×10^4
Coloane	50	10	15	0.88	0.44×10^4
Total land area of Macao	566	120	168	9.42	3.37×10^4

Table 7. Simulated average contributions contributed by primarily vehicular emissions in Macao, weekdays during November 2010

Region / Parish	Simulated concentrations of primary vehicular emissions ($\mu g\ m^{-3}$)					
	CO			PM$_{2.5}$		
	Mean	Min	Max	Mean	Min	Max
Macao Peninsula	199	57.8	415	2.03	0.67	3.89
St. Lazarus Parish	330	270	415	3.14	2.59	3.89
St. Lawrence Parish	180	139	265	1.72	1.32	2.47
Our Lady Fatima Parish	171	77.8	209	1.64	0.67	3.21
St. Anthony Parish	296	223	362	2.85	2.17	3.39
Cathedral Parish	166	57.8	370	2.03	1.00	3.14
Taipa	42.1	12.6	104	1.65	0.61	2.46
CoTai Reclamation Area	37.1	11.2	63.1	1.08	0.27	2.39
Coloane	16.9	7.0	54.1	0.29	0.12	0.63
Total land area of Macao	84.5	7.0	415	1.30	0.12	3.89

Note: Simulated results for November 6-8 are not accounted in this table due to the impact of rainfall. Mean, minimum and maximum values are for simulated average concentrations of each receptors in each region/parish during the study period.

1 **Figures**
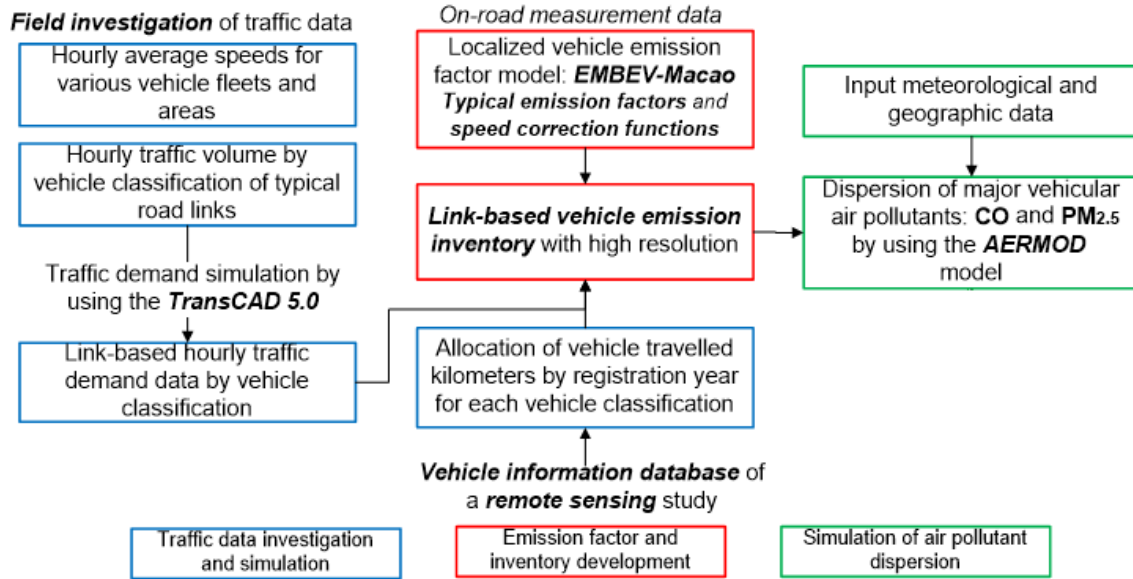
3 Fig. 1. Framework of high-resolution simulation for vehicle emissions and concentrations
4 of vehicular pollutants.
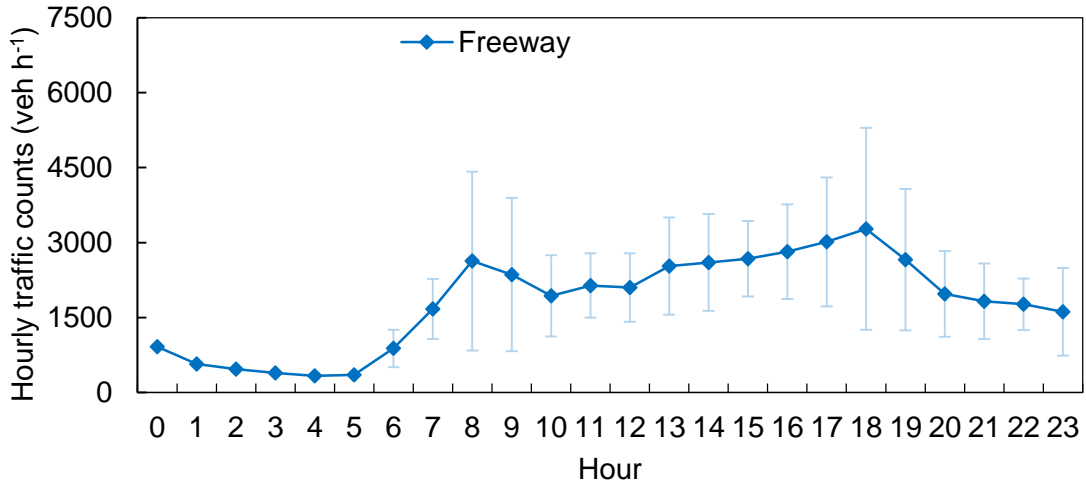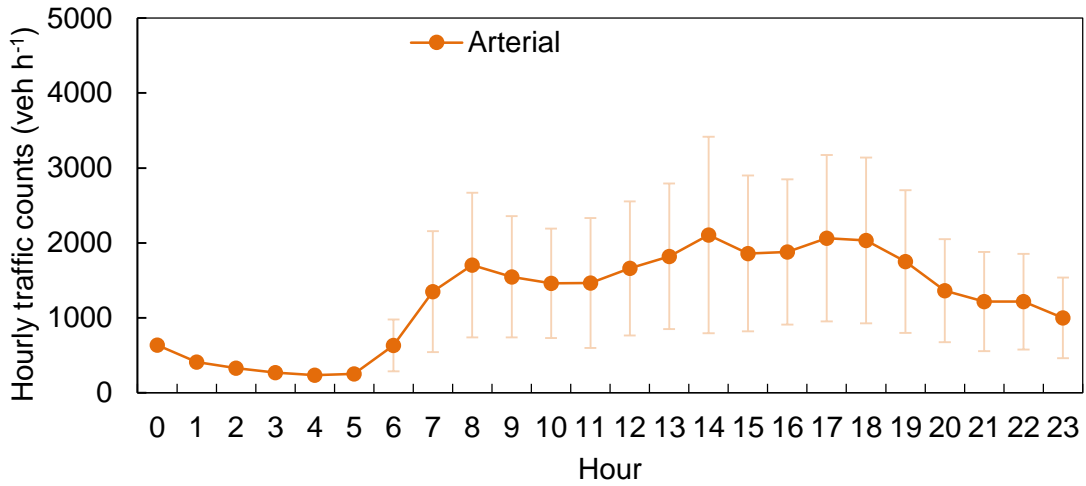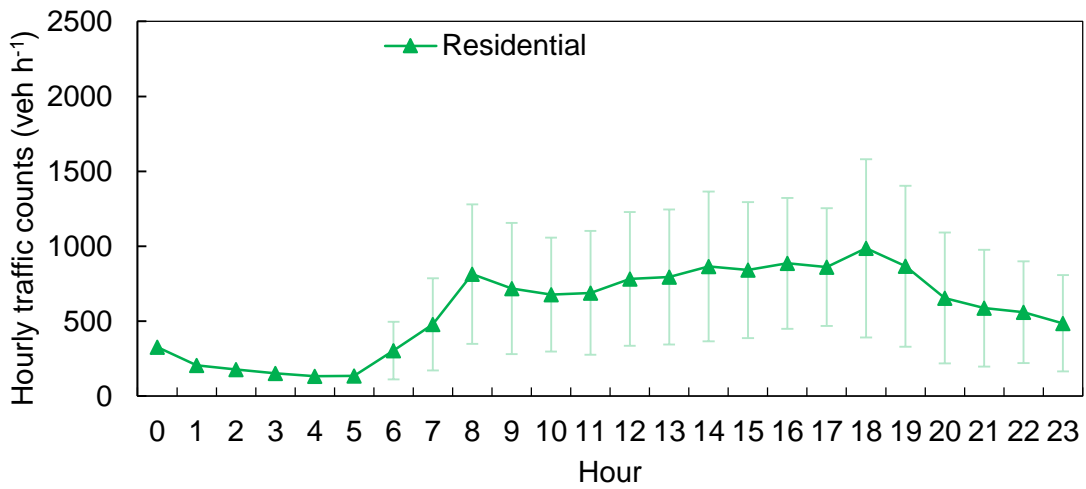
4   Fig. 2. Mean hourly traffic accounts of observed links by road class during weekdays, 2010.
5   The error bars indicate standard deviations of observed data, from 6 a.m to 11 p.m.
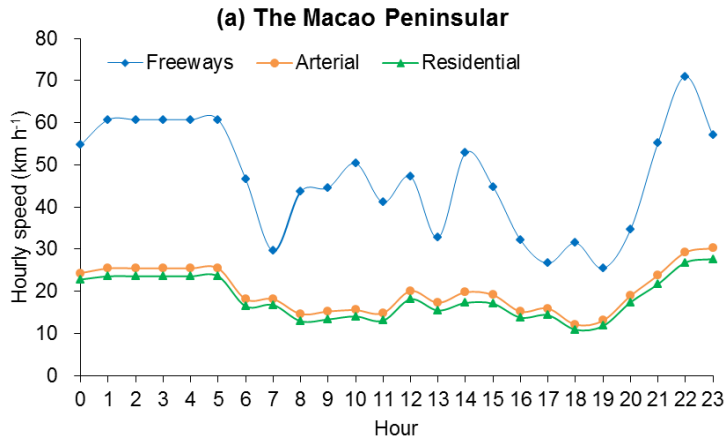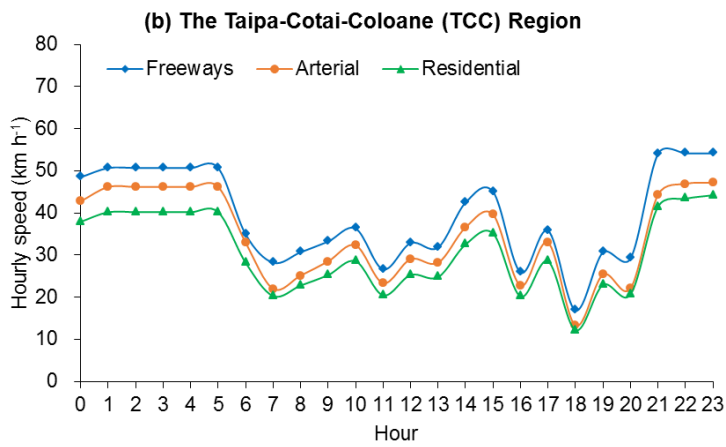
4
5 Fig. 3. Variations in aggregated hourly speeds by road class and region for LDPVs during
6 weekdays, 2010.
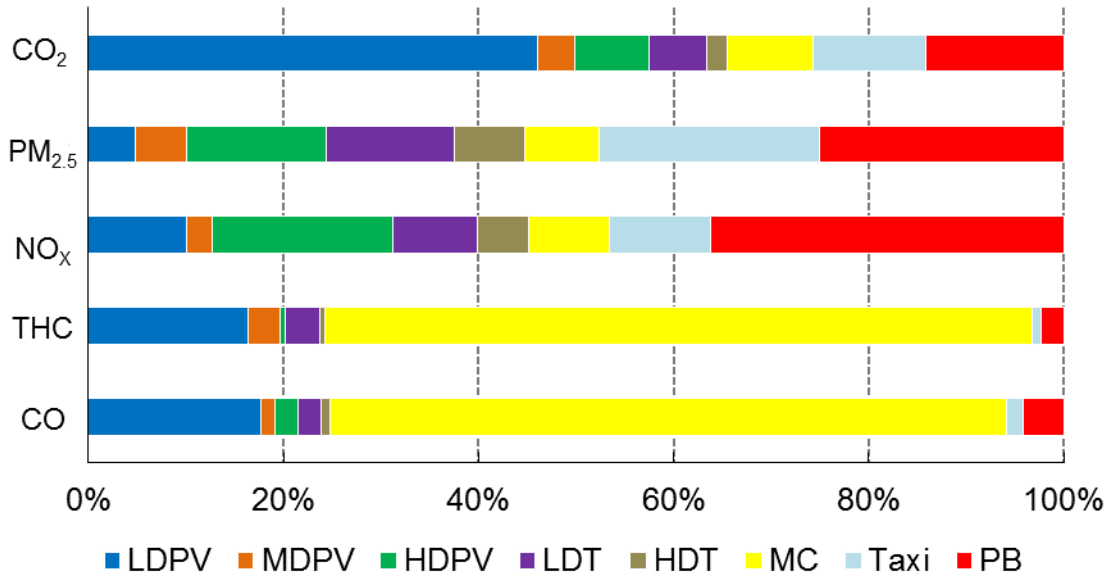
2 Fig. 4. Allocations of total vehicular emissions by vehicle classification
3
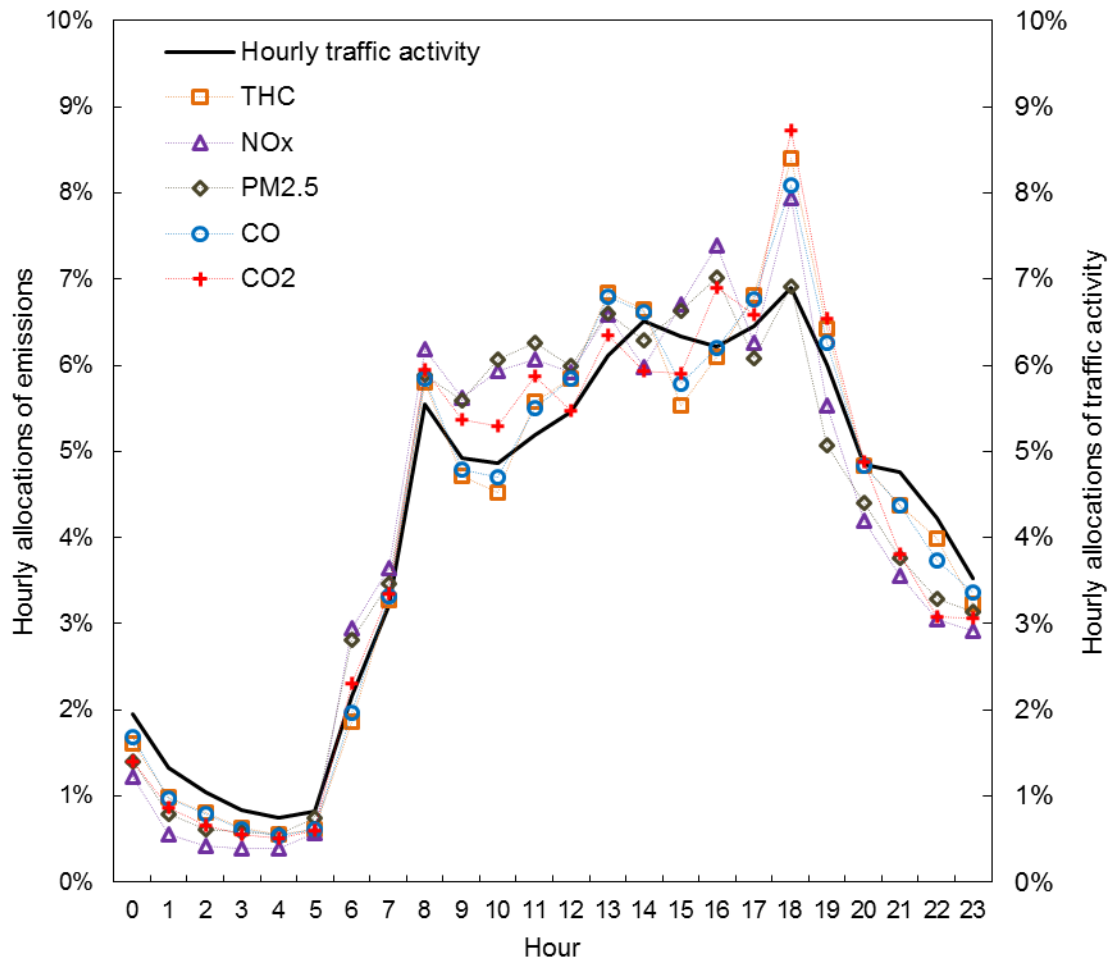
2 Fig. 5. Hourly allocations of vehicular emissions and traffic activity in Macao during
3 weekdays, 2010.
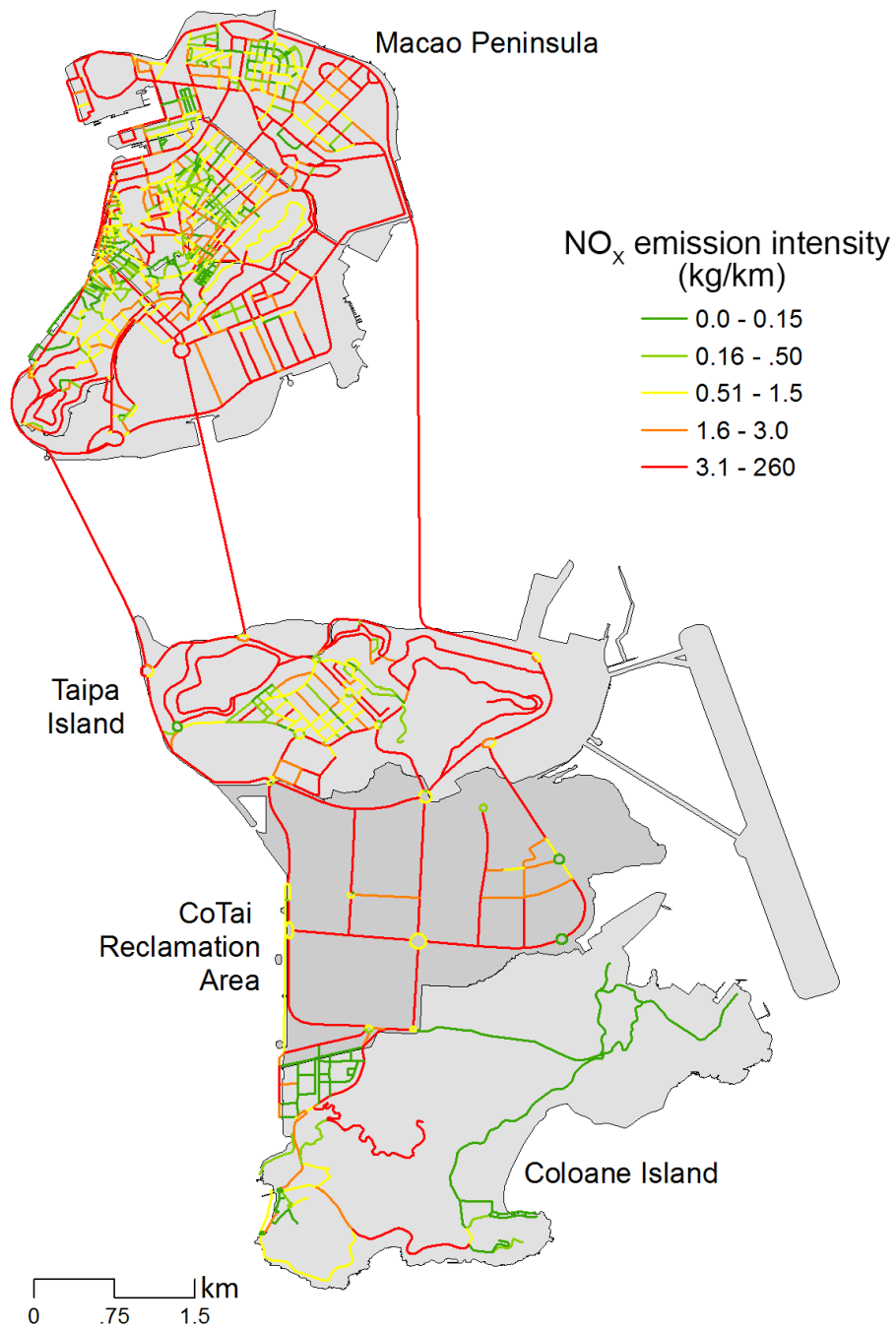
2   Fig. 6. The spatial distribution of NO_X emission intensity for on-road vehicles in Macao
3   during a typical weekday of 2010
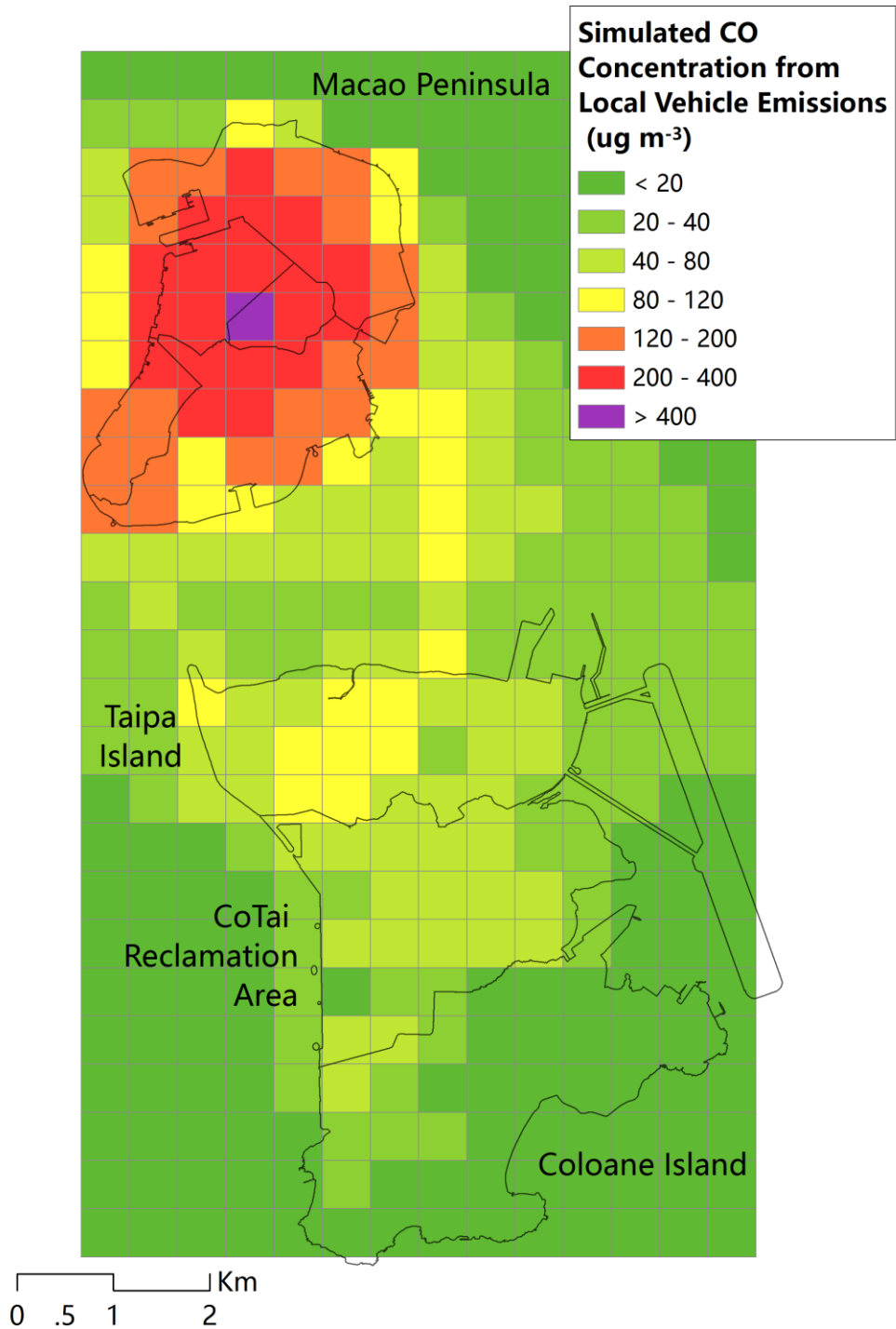
2   Fig. 7. Simulated vehicle-contributed concentration of CO in Macao during weekdays of
3   November, 2010
4